THÜNEN

Institute of Baltic Sea Fisheries (OF)

Alter Hafen Süd 2, 18069 Rostock Fon +49 381 66099-122 Fax +49 381 6609-199 Date 25.01.2021 E-Mail: juan.santos@thuenen.de

Cruise Report
FRV „Solea" Cruise 797
15.– 30.09.2021

Scientists in charge: Juan Santos

In a nutshell

Fishing trials conducted during the Solea cruise N° 797 were devoted to fundamental research on codend selectivity. Based on a novel experimental setup involving codends with mesh geometries fixed to a specific opening angle (OA), the main aim of the research was to isolate and quantify the effect of the variability of mesh opening angles (OA) on the selectivity of Baltic demersal fish species. Fishing trials were conducted in the central-south Baltic Sea between the 16 and 29 of September 2021. Codend selectivity data was collected using the cover-codend method. Flatfish species dominated the catches, while catches of cod were scarce. The low catches of cod led to a reduction in the original experimental plan. Therefore, only two of the five experimental codends available were finally tested: i) an experimental codend with mesh geometry fixed to an OA of 40° (OA40) and ii) a standard diamond-mesh codend with the mesh geometry subjected to variation (OA not fixed). Preliminary results reveal that the variation in mesh geometry associated to standard codends negatively impacts on the sharpness of the selectivity curve for cod, leading to 45% significant wider selection range (SR) than the SR estimated for the AO40 codend. In contrast, variation in mesh geometry did not significantly influenced the selectivity of flatfish species. The experimental results obtained in this cruise validate theoretical predictions regarding the influence of variation in mesh geometry on the selectivity of cod and flatfish species. The current investigation should be resumed with additional sea trials to assess the selectivity of the remaining experimental codends.

Distribution list:

Ship management FFS „Solea"
BA für Landwirtschaft und Ernährung (BLE) Fischereiforschung
BM für Ernährung und Landwirtschaft (BMEL), Ref. 614
BA für Seeschifffahrt und Hydrographie (BSH), Hamburg
Deutscher Angelfischerverband e.V.
Deutsche Fischfang-Union, Cuxhaven
Deutscher Fischereiverband Hamburg
Doggerbank Seefischerei GmbH, Bremerhaven
Erzeugergemeinschaft der Deutschen Krabbenfischer GmbH
Euro-Baltic Mukran
Kutter- und Küstenfisch Sassnitz
LA für Landwirtschaft, Lebensmittels. und Fischerei (LALLF)
LA für Landwirtschaft und Fischerei MV (LFA)
DTU-Aqua - Danish Institut for Aquatic Resources
Leibniz-Institut für Ostseeforschung Warnemünde
GEOMAR Helmholtz-Zentrum für Ozeanforschung Kiel
Thünen-Institute - Institute of Fisheries Ecology
Thünen-Institute - Institute of Sea Fisheries
Thünen-Institute – Institute of Baltic Sea Fisheries
Thünen-Institute – Press office, Dr. Welling
Thünen-Institute – Presidential office
Thünen-Institute – Scheduling research vessels, Dr. Rohlf

1 Introduction to the Research Topic

In the Baltic Sea demersal trawl fisheries, adjusting the selectivity of the codend is the most applied strategy to avoid the bycatch of juvenile cod (Madsen, 2007). This is generally intended by adjusting the size and openness of the meshes considering the body size and shape of the species subjected to selection (Wileman *et al.*, 1996; Millar and Fryer, 1999; Pope *et al.*, 1975; Wienbeck *et al.*, 2011).

Codends are flexible devices subjected to different mechanical forces during the fishing operations. Such forces act on the codend netting altering the geometry and openness of the meshes (Herrmann *et al.*, 2007; Pichot *et al.*, 2009). In theory, variations in the geometry of the meshes can potentially lead to a wide range of size selection signatures. Therefore, the probability associated to an attempt to escape will be dependent on to which specific mesh geometry the fish contacted to. Following this rationale, the size selection of the codend that generates the selectivity data obtained at the end of a fishing haul can be interpreted as an average of available size selection curves associated to different working geometries of the codend meshes during this specific haul.

The size selection of trawl codends is traditionally described using mathematical functions with functional forms controlled by (at least) two parameters, the L50 (the fish length with 50% probability of being retained in the codend) and Selection Range (SR, the range of lengths between lengths with 75% and 25% retention probability) (Wileman *et al.*, 1996). While the L50 parameter controls the position of the retention curve relative to the range of sizes of the population of fish exploited, the SR parameters control the steepness of the curve. Therefore, large SR values relate to flat selection curves, while small SR values lead to a sharp selection. Based on computer simulations, Herrmann (2005) theorized that variations in mesh geometry resulting from towing forces and catch accumulation can be a major contributor for the SR. If the hypothesis arising from the theoretical study in Herrmann (2005) is true, the more the variation in mesh geometry, the larger the SR and the poorer the definition of the selection curve. Conversely, the more stable the mesh opening during the fishing operations, the sharper the resulting selection curve will be based on the theoretical investigations.

Despite the huge efforts devoted in the last decades on codend selectivity research, there are still fundamental uncertainties and open questions regarding how fish is mechanically selected. Isolating and quantifying the underlying contributors to the SR of the codend could improve the fundamental knowledge on codend selectivity while open conceptual paths towards new codend designs able to provide more sharp and stable size selection than the current concepts. Therefore, the main aim of the Solea cruise N° 797 was to quantify the effect of variations in the mesh geometry on codend size selection, and more specifically how much such variation impacts on the steepness of the selection curves from traditional diamond-mesh codends.

2 Material and Methods

2.1 Fishing gears

The original cruise plan involved testing the selectivity properties of five different codend designs made of the identical netting material (Table 1). Designs D2 and D4 are standard T0 (diamond-mesh) and T45 (square-mesh) codends to represent the variability in mesh openings that could be encounter in commercial fishery. Designs D1 ,D3 and D5 are designed to keep the opening angle of the meshes fixed respectively at 40° (D1, diamond-mesh), 60° (D3, diamond-mesh) and 90° (D4, square-mesh). The fixation of the opening angles was achieved by attaching the netting with specific hanging ratios to a 2 x 0.75 x 0.75 m (1.125 m^3) rigid box frame made of steel (Figure 1) The five experimental codends were designed by the Danish partners and produced by the netmaker company Cosmostrawl (Hirtshals, Denmark).

Table 1 Technical specifications of the experimental codends taken onboard, listed according to the sequence of tests originally planed. Designs tested during the cruise in bold. Mesh measurements taken according to Fonteyne et al. (2007), standard deviation of the mesh measurement sample (n=20) in brackets.

ID Experiment	Mesh Angle (degree)	ID Design	Netting orientation	mesh size (mm)
D1	**Fixed 40°**	**OA40**	**T0**	**111.5 (2.14)**
D2	**Variable**	**T0**	**T0**	**112.4 (2.72)**
D3	Fixed 60°	OA60	T0	-
D4	Variable	T45	T45	-
D5	Fixed 90°	OA90	T0	-

Figure 1: Rigid frames (two units stacked) used to fix the mesh geometry at OA = 40°, 60° and 90°.

In order to compensate for the negative flotation caused by the constructive material of the rigid frame, one line with 7x foam buoy floats was attached to each longitudinal upper bars of the device (Figure 3). The codends were shipped from the production site to the Thünen Institute of Baltic Sea Fisheries (Rostock) in September 14, one day before the start of the cruise (Figure 2).

The experimental codends were connected to a trawl model TV300/60 by a 4-meters extension piece (stretchered length) made of small mesh (50 mm nominal mesh size). This mesh size was considered non-selective for the species and length classes of research interest. Therefore, the total length of the extension piece and the rigid codend was 6 m. The trawl was spread by two doors Thyboron Type 2 (1.78 m^2) and 100 m sweeps.

Figure 2: Side view of codends D1 (OA40, top) and D3 (OA60, bottom).

2.2 Data Collection and sampling procedures

The cover method

Escapees resulting from the size selection of the experimental codends (*CD*) were collected using the cover-codend method (Wileman *et al.*, 1996; Wienbeck *et al.*, 2011, 2014). The cover (*CC*) is made of single 2.5 mm-PE twine and a nominal mesh size of 55mm, it has a stretched length of ~16 m (2.6 x the length of the extension piece and rigid codend combined) and a diameter of ~3 m. In order to prevent the cover from masking the selectivity of the codend, a total of seven kites were attached to the cover, in order to keep a stable and sufficient physical separation between both compartments. Five kites were attached to the forward section and the remaining two were attached two each side of the cover (Figure 3). The catches obtained at haul level were sampled for each compartment and fish species separately.

Figure 3: Lateral view of the experimental OA40 codend surrounded by the cover. The cover was rigged with forward (red, green and grey) and lateral kites aligned to the mid-length of the codend (grey). To compensate for the negative buoyancy of the OA40 codend, the device was initially rigged with 2x floating lines consisting of 7x foam buoys that were attached side by side along the longitudinal upper bars of the frame.

Catch sampling

Catches obtained in the test codend and the cover codend at haul level were sampled separately by species. When possible, all fish were length-measured. In case of excessive catches of a given species, a random sub-sample was obtained from the total, and the ratio of subsampled weight to the species total catch weight was calculated as sampling factor. Specific sampling schemes were applied to relevant flatfish species (plaice, flounder, dab) and roundfish (cod and whiting). The sampling scheme applied to roundfish individuals included measurements of total length (cm below), circumference of the cross section at the point of maximum width of the head (CS1, [mm]), and the circumference of the cross section of the maximum body height and width (CS2 [mm], Figure 4) (Herrmann *et al.*, 2009). Length measurements of flatfish individuals included total length (cm below) and maximum body width (mm, dorsal and anal fins compressed, Figure 4). The sampled individuals were individually weighted (gram) using electronic scales.

Provided that the hypothesis in Herrmann (2005) regarding the large impact of variability of mesh openings on the selection range is true, having fixed opening angles in D1, D3, and D5 (Table 1) would allow investigating other individual traits potentially influencing codend selectivity, without the potential confounding related to the flexible nature of a standard codend. It is of particular interest to investigate if individual fish traits others than body length can be related to the retention probability. Therefore, the traditional sampling conducted on length measurements (Wileman et al. 1996) was extended by the collection of additional biological traits from cod individuals larger than 20 cm:

- Maturity state (BITS index)
- Gallbladder state (BITS index)
- Stomach fullness (BITS index)
- Nematods (BITS index)
- Sex
- Gutted and ungutted weight
- Liver weight

This sampling scheme was applied to cod sub-samples obtained separately from the codend catches (retained fish) and the cover (escaped fish). The BITS index refers to ordinal traits used in Baltic International Trawl Survey (BITS) to determine the biological status of fish populations.

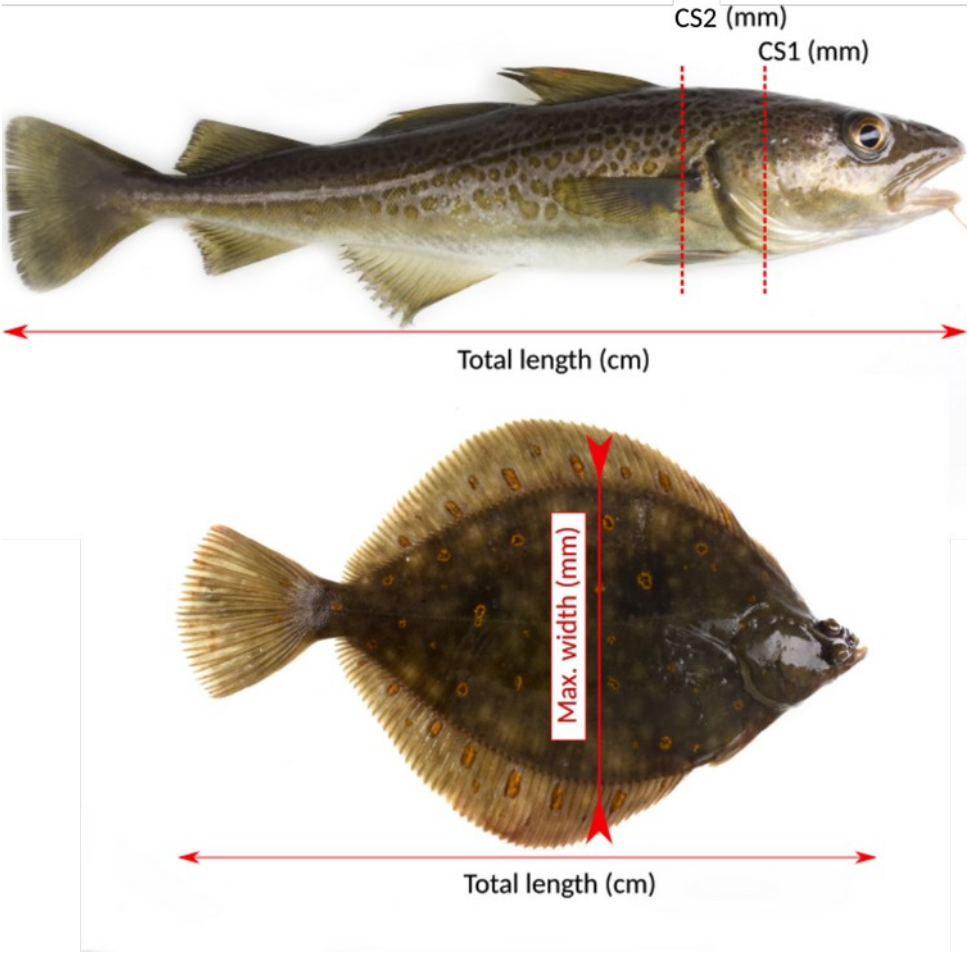

Figure 4: Morphological measurements taken for cod and flatfish species (plaice, flounder and dab).

2.3 Selectivity analysis

Estimation of codend selectivity

The size selection delivered by each of the experimental codend was analyzed by species using the traditional methodology described in Wileman et al. (1996). The traditional codend-selectivity

analysis assumes that (a) the proportion of the fish retained in the codend is determined by the ability of the fish to pass through the codend meshes, and (b), that such ability is determined mostly by the morphology and size of the fish, and the meshes' geometry and size. These basic assumptions allow modeling the codend retention probability *r(l)* by simple mathematical functions with parametric structures leading to non-decreasing, s-shaped selectivity curves (Figure 5) asymptotically restricted to values between [0, 1] (Wileman *et al.*, 1996; Millar and Fryer, 1999) The most often applied selectivity functions are the logistic, *probit*, *gompertz*, and *Richards:*

$$r(l,\mathbf{v}) = \begin{cases} logistic = \frac{exp(\frac{ln(9)}{SR}\times(l-L50)}{1+exp(\frac{ln(9)}{SR}\times(l-L50)} \\ probit \approx \Phi\left(1.349 \times \frac{(l-L50)}{SR}\right) \\ gompertz \approx exp\left(-exp\left(1.573 \times \frac{(l-L50)}{SR} - 0.366\right)\right) \\ Richards = \left(\frac{exp\left(logit(0.5^{\delta})+\left(\frac{logit(0.75^{\delta})-logit(0.25^{\delta})}{SR}\right)\times(l-L50)\right)}{1.0+exp\left(logit(0.5^{\delta})+\left(\frac{logit(0.75^{\delta})-logit(0.25^{\delta})}{SR}\right)\times(l-L50)\right)}\right)^{\frac{1}{\delta}} \end{cases} \quad \text{(Eqs. 1)}$$

Where ***v***=(L50, SR). Note that the *Richards* function involves an additional parameter δ to add flexibility to the functional form.

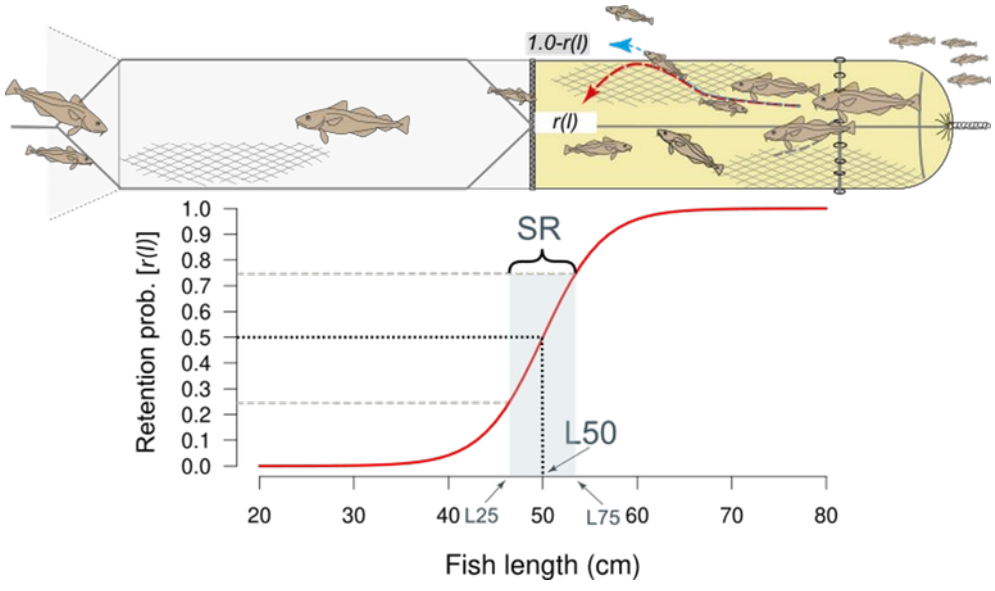

Figure 5. Top: representation of a size-selection process in the codend. Bottom: example of a retention curve describing codend retention probability, with associated parameters L50 and SR. The notation referred to retention curve r(l) in the figure is an abbreviation of r(l,L50,SR) in text.

In a size selection process, it can be hypothesized that a fraction of fish that enter the codend might not make an efficient contact with the mesh openings, and consequently those individuals will not be subjected to size selection. To cope with this situation, traditional size-selection models can be extended by introducing an additional parameter that accounts for the fraction of the fish that having entered the codend contacted the meshes becoming available for size selection. The sequence of these two probabilistic events defines the length-dependent contact retention (Millar and Fryer, 1999; Sistiaga *et al.*, 2010):

$$r_c(l, \mathbf{v}) = C \times r(l, \mathbf{v}) \qquad \text{(Eq. 2)}$$

where the parameter *C* quantifies the fraction of the fish that contacted the mesh opening, and *r(l)* represents the available size selectivity in the codend described by any of the functions presented in Eqs. 1.

Another valid assumption to describe size selection of a codend is the co-existence of more than one average size selection signature. In the case of assuming a dual selection process, then it should be expected that a fraction of fish entering the codend will be available to one of the size selection signatures, while the remaining fish will be selected by the other size selection signature. This process can be mathematically described by extending Eq. 2:

$$r_{s2}(l, \mathbf{w}) = C \times r_1(l, \mathbf{v}_1) + ((1.0 - C) \times r_2(l, \mathbf{v}_2)) \qquad \text{(Eq. 3)}$$

Where $\boldsymbol{v_1}$ and $\boldsymbol{v_2}$ are the vectors of selectivity parameters defining the two size selection processes considered, and $\boldsymbol{w = (v_1, v_2)}$. The experimental method applied in this study enables collecting the retained and escaped fish of length *l* respectively in the codend (ncd_l) and the cover (ncc_l). The direct observation of retained and escaped fish allows estimating the models described in Eqs. 1,2 and 3 and associated selectivity parameters by minimizing the negative of the log-likelihood of the following binomial probability mass function:

$$-\sum_i \sum_l (ncd_{il} \times log(r(l)) + ncc_{il} \times log(1.0 - r(l)) \qquad \text{(Eq. 4)}$$

Being *r(l) any of the selectivity models presented in Equations 1,2 or 3*. Eq. 4 introduces the summation over hauls $h \in \{i=1,\ldots,m\}$, being ncd_{il} and ncc_{il} the fish sampled at haul *i*. Thus, assuming that the *m* hauls were randomly drawn from all possible hauls that could be conducted, Eq. 4 returns an estimate of the population-average selectivity properties of the codend tested. All models described in Eqs. 1,2 and 3 were estimated and ranked by AIC (Akaike, 1974), and the best candidate model was picked for further analysis.

Evaluation of differences in selectivity among tested codends

The main aim of the research is to assess if fixing the mesh geometry of the codend to a given opening angle (OA) has a significant effect on codend selectivity, in particular to the curve steepness, which is related to the selectivity variability occurring within-and between haul. Thus, considering the selectivity of the D2 codend a reference for the selectivity provided by standard codends, the following statistic was considered:

$$\Delta SR = SR_{D2} - SR_{D1} \qquad \text{(Eq. 5)}$$

Eq. 5 quantifies the absolute differences in the SR estimated for the codend design D2 relative to D1. In order to assess if the value of ΔSR is significantly different to zero, the 95% percentile confidence intervals are estimated from the bootstrap distribution of ΔSR, which is obtained from the bootstrap distributions of SR_{D1} and SR_{D2} previously obtained :

$$\Delta SR^{*b} = SR^{*b}_{D2} - SR^{*b}_{D1} \qquad \text{(Eq. 6)}$$

Uncertainties in the estimation of the different statistics presented in this report, derived from the limited sampling size and between-haul variation was accounted by applying the bootstrap method firstly implemented by Millar (1993). The bootstrap distributions of the different parameters were used to estimate 95% percentile confidence intervals.

3 Cruise narrative and preliminary results

3.1 Initial settings

The sampling material and fishing gears were taken onboard during the first day of the cruise (15.09). The crew connected the OA40 codend (Figure 3) and the cover-cover to the trawl at the pier. To neutralize the negative buoyancy of the steel frame, the OA40 codend was initially rigged with 2x floating lines consisting of 7x foam buoys, attached side by side along the longitudinal upper bars of the frame. Fishing trials started the next day (16.09) at fishing grounds of Warnemünde/Kühlungsborn (ICES SD22-24). Underwater video recordings collected in every haul of this preparatory first day were used to assess the hydrodynamic and mechanic behavior of the experimental gear. In particular, it was important to check that there was enough space between the codend and the cover, and that the codend did not flip over during towing. Videos from haul 1 confirmed high stability of the codend, and a sufficient interstitial space between the codend and the cover codend (Figure 6). However, the video observations also revealed excessive codend buoyancy. Consequently, it was decided to reduce the number of foam floats from 2x7 to only 2x3. Besides gear setup procedures, this first day was used to gain experience on how to handle the experimental gear and its steel frames during shooting and heaving maneuvers.

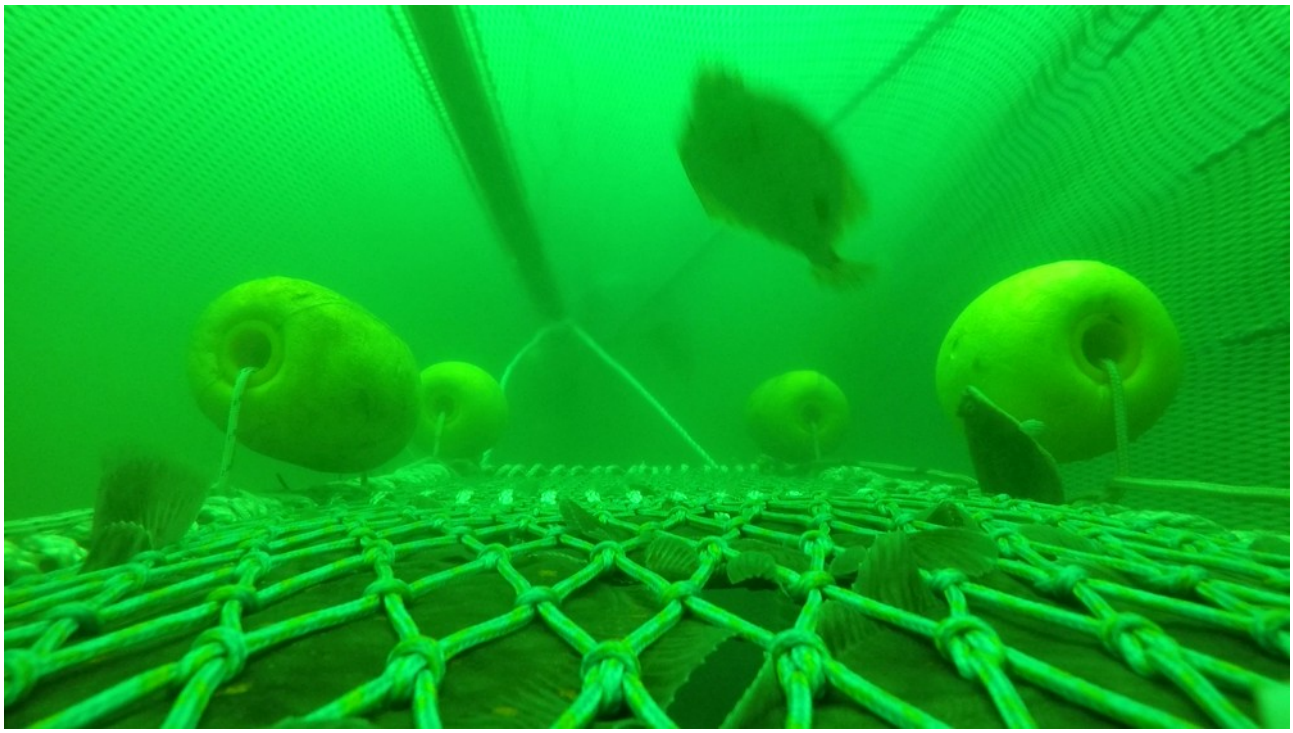

Figure 6: Image taken from a UW camera mounted outside of the upper panel of the OA40 codend. The camera was placed at the rear of the codend to provide a view forwards (against the towing direction). The image reveals a sufficient Interstitial space between codend and cover. Flatfish positioned beneath the top panel obstructing the meshes, and two individuals escaping.

3.2 Fishing operations and catches

Altogether, 55 experimental hauls were conducted in a total of 12 fishing days from 16 to 27 of September, covering a wide spatial area within ICES 22-24, with the most western hauls conducted off the coast of Kühlungsborn (54°14.6N, 11°47.7E), and the most eastern hauls in shallow waters in east of the Island of Rügen (54°21.0N, 14°00.7E).

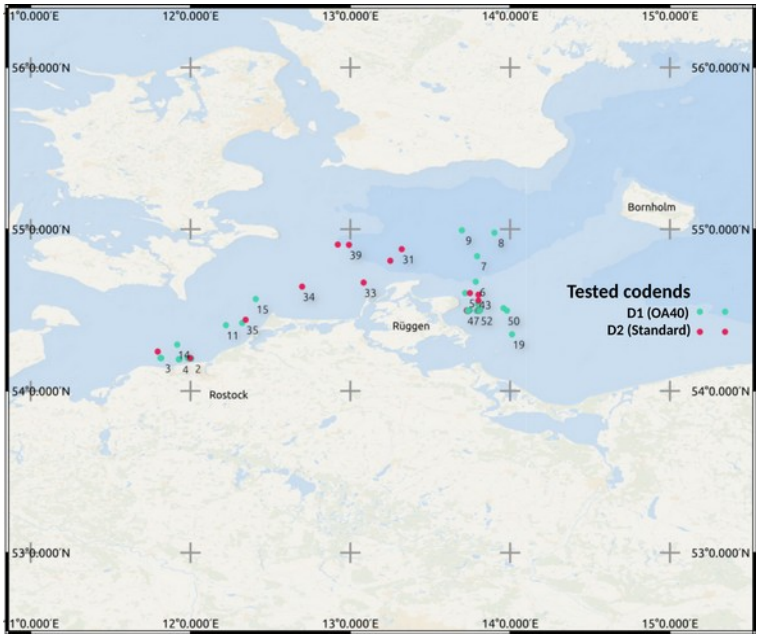

Figure 7: Spatial distribution of the experimental hauls

During the entire cruise, catches were generally rather small. Flatfish species dominated the catches throughout the cruise. Among the most relevant species, the most caught one was flounder (FLE; *Platitchthys flesus*, 41.60 ± 4.72 kg/haul), followed by plaice (PLE; *Pleuronectes platessa*, 23.66 ± 4.52 kg/haul) and dab (*Limanda limanda*, 6.82± 2.34 kg/haul). The abundances of flounder and dab were strongly correlated to fishing areas; while dab and plaice were the most caught species in the western hauls (Warnemünde-Kühlungsborn), flounder and plaice made up the catches in eastern hauls (Figure 8, Table 4). Catches of cod (2.37± 0.55 kg/haul) and withing (0.13± 0.06 kg/haul) were scarce. The low abundance of cod encountered (catches with more than 100 cod individuals only occurred in hauls 17 and 45, Figure 8, Table 4) forced a continuous, yet unsuccessful search for higher abundances across fishing grounds forced a continuous, yet unsuccessful search for higher abundances across fishing grounds (Figure 7) and fishing depths (19 – 46 m). Overall 18 out of 55 hauls took place in a small fishing area in front of Sassnitz (Rüggen island), where a weak signal of cod occurred. As the catches of cod did not improved, it was decided to reduce the initial experimental plan (Table 1), and only the codend designs D1 (OA40 , 32 hauls) and D2 (Standard T0 codend, 23 hauls) were tested. By focusing the sampling effort available to only two codend design, it was intended to maximize the power of the pooled catch data for the assessment of a potential effect of the variability of mesh opening angles on cod selectivity.

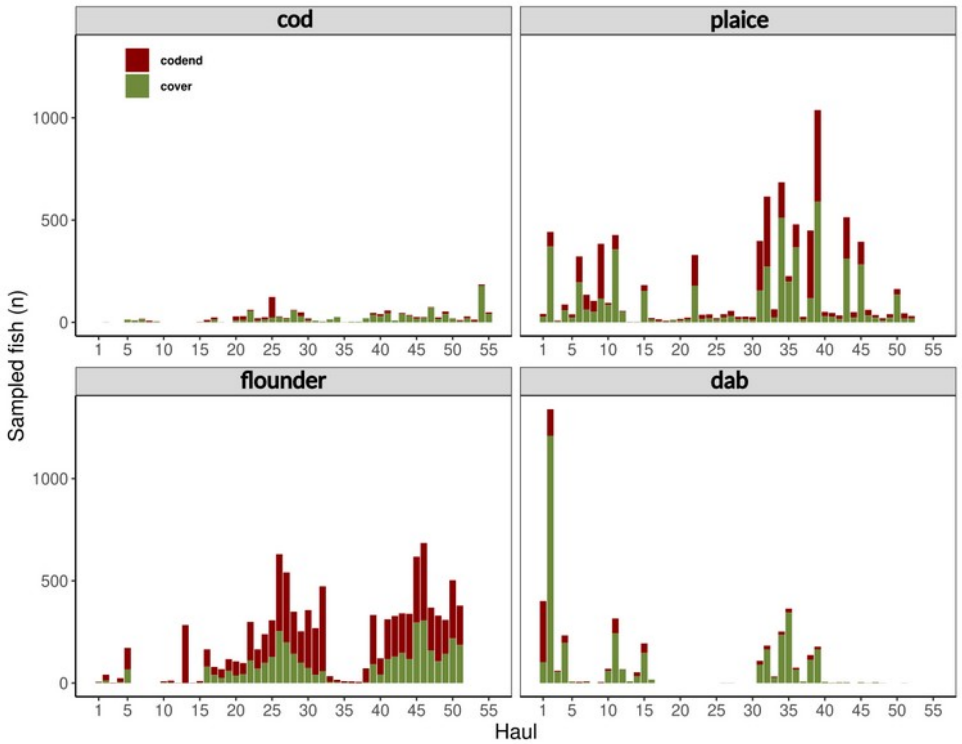

Figure 8: Catch numbers by compartment, haul and species. Only the four most caught species shown.

3.3 Preliminary results

The present document only provides preliminary results related to the main research topic addressed during the cruise. Therefore, only size selection analysis based on fish total length are presented. Additional data on selectivity depending on individual fish traits has been explored but not analyzed at the time of writing this document.

The selectivity of the two tested codends was successfully estimated for all the analyzed species. The best candidate model for cod selectivity data was the logistic model described in Eqs. 1. The selectivity of plaice from both codends and dab selectivity from D1 were best described by a dual-selection model involving two logistic functions (Eq. 3). Dab selectivity from D2 codend and flounder selectivity from D1 and D2 were best described by a contact model (Eq. 3) with the Richard function describing the length-dependent component. A visual inspection of the resulting size selection curves for cod show relative large differences between the two tested codends (Figure 9). In contrast, the same pairwise comparison applied to flatfish species reveal very little discrepancies, which is visually expressed by a full overlap of the confidence intervals across the range of available lengths (Figures 10 - 12). For cod, the evaluation of differences in selectivity among tested codends based on the ΔSR statistic reveal that the variation in mesh geometry associated to standard codend (D1) significantly impacts on the sharpness of the selectivity curve for cod. In particular, the SR of the standard codend (D2) was 45% wider than the SR estimated for the AO40 codend (~ 2.6 cm lower, in absolute terms, Figure 13). In contrast, variation in mesh geometry did not significantly influenced the selectivity of flatfish species Table 2, Figure 13.

Table 2: Selectivity parameters and fit statistics associated to the selectivity models for the species analyzed, estimated based on by-species selectivity data obtained with the T0 and AO40 codends. The species-specific models presented were picked from a list of candidate models by AIC.

Codend	D1 (Standard T0 codend)				D2 (Fixed-mesh codend, OA40)			
Species	COD	PLAICE	DAB	FLOUNDER	COD	PLAICE	DAB	FLOUNDER
Model	*Logistic*	*LogisticS2*	*LogisticS2*	*CRichard*	*Logistic*	*LogisticS2*	*CRichard*	*CRichard*
L50	**27.79 (25.19-30.67)**	24.51 (23.91-25.03)	26.94 (26.01-27.59)	23.68 (23.19-24.17)	**23.42 (22.24-25.01)**	24.97 (24.14-25.65)	27.11(26.78-27.63)	24.28(23.69-24.79)
SR	**8.75 (6.75-11.57)**	2.18 (1.54-3.25)	1.94 (0.59-4.99)	3.62 (2.73-4.96)	**6.04 (4.70-7.65)**	1.77 (1.01-2.63)	1.88 (1.36-2.50)	3.85 (2.96-5.34)
P-value	0.17	0.18	1	0.05	0.58	0.15	0.06	0.63
Deviance	38.56	36.82	5.31	40.58	30.82	32.11	33.03	26.00
DOF	31	30	20	27	33	25	22	29

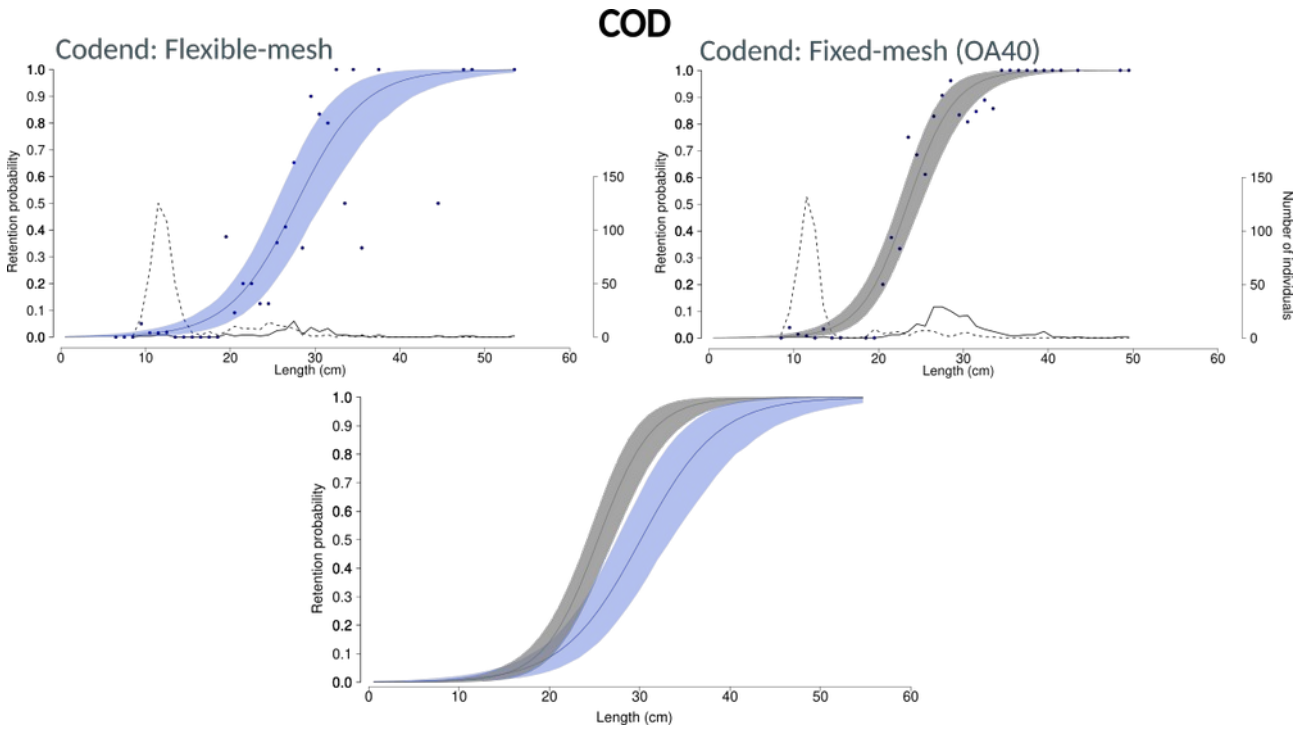

Figure 9: Average selectivity curves and associated 95% confidence bands obtained for cod using the flexible-mesh (top left) and fixed-mesh (top right) codends. The lines represent the length distribution fish in the experimental codend (solid line) and the cover codend (stipled line). Bottom: both curves and related confidence bands plotted together for comparative purposes.

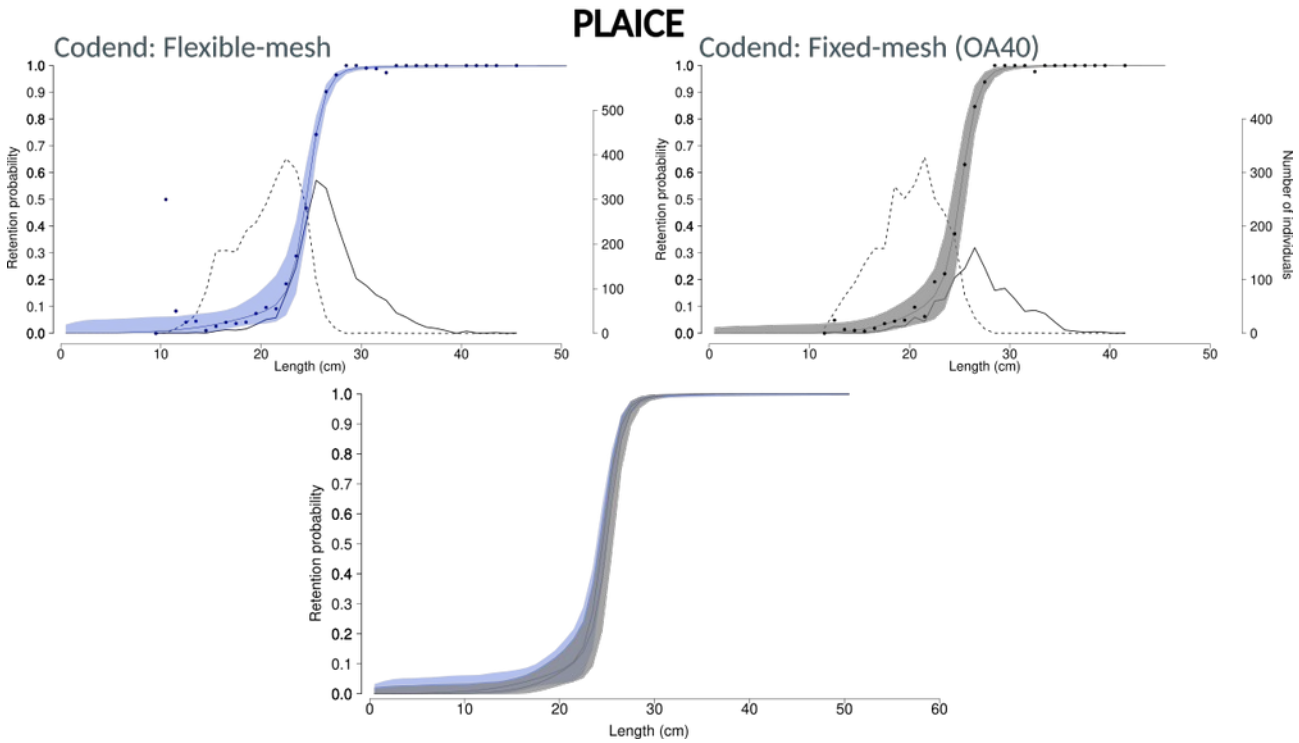

Figure 10: Average selectivity curves and associated 95% confidence bands obtained for plaice (PLE) using the flexible-mesh (top left) and fixed-mesh (top right) codends. The lines represent the length distribution fish in the experimental codend (solid line) and the cover codend (stipled line). Bottom: both curves and related confidence bands plotted together for comparative purposes.

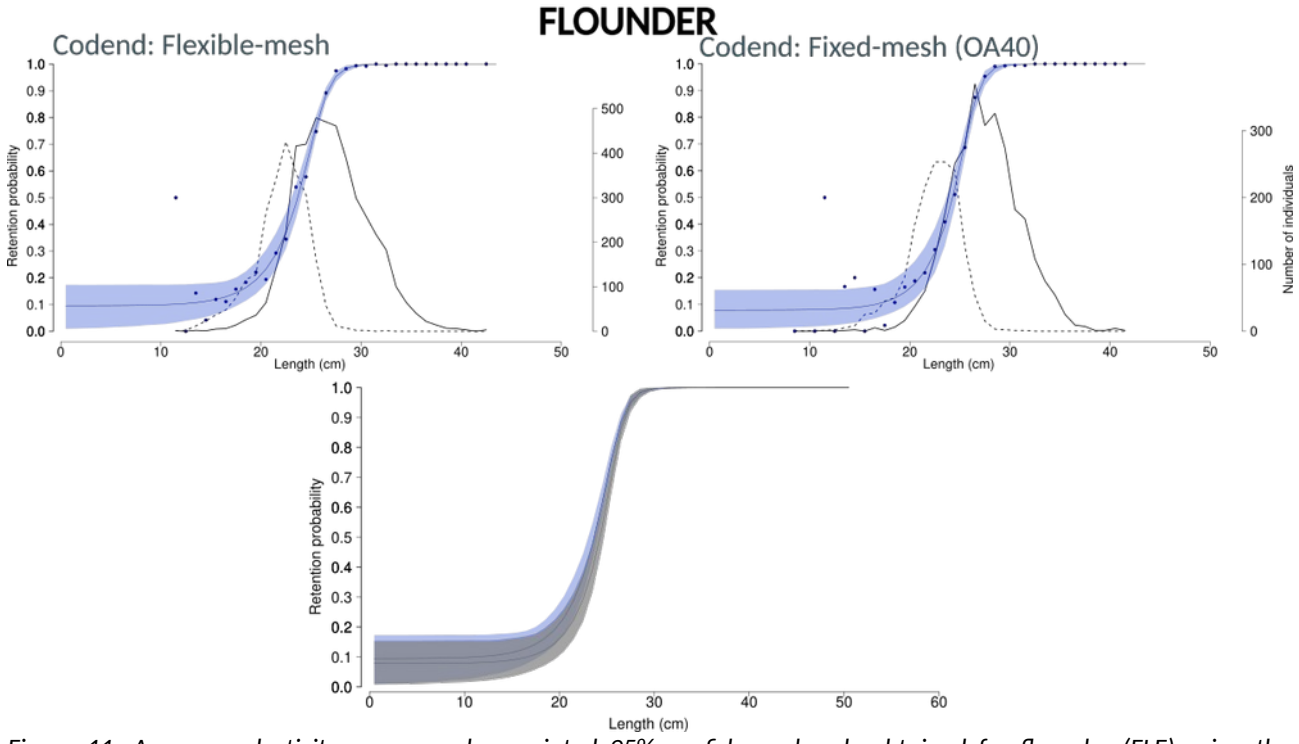

Figure 11: Average selectivity curves and associated 95% confidence bands obtained for flounder (FLE) using the flexible-mesh (top left) and fixed-mesh (top right) codends. The lines represent the length distribution fish in the experimental codend (solid line) and the cover codend (stipled line). Bottom: both curves and related confidence bands plotted together for comparative purposes.

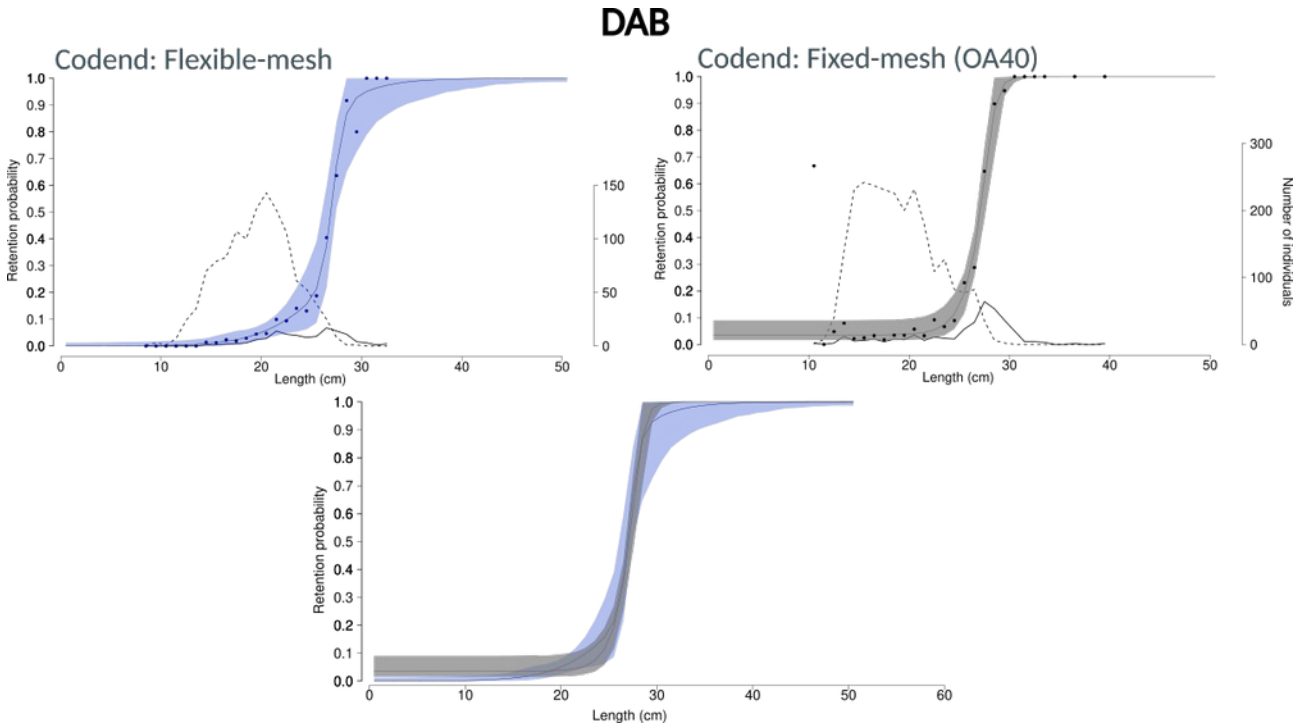

Figure 12: Average selectivity curves and associated 95% confidence bands obtained for dab using the flexible-mesh (top left) and fixed-mesh (top right) codends. The lines represent the length distribution fish in the experimental codend (solid line) and the cover codend (stipled line). Bottom: both curves and related confidence bands plotted together for comparative purposes.

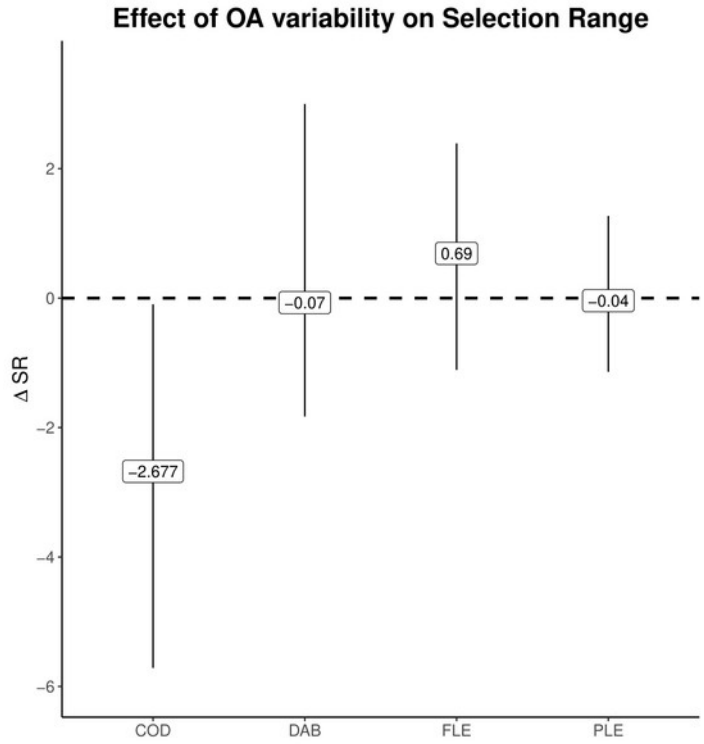

Figure 13: Bias-corrected absolute differences in SR value obtained with the fixed-mesh codend relative to the SR from the flexible-mesh codend. Significant differences only found for the case of cod.

4 Final remarks

The experiment conducted during the 797 Sole cruise has been designed to quantitatively investigate the effect of variation in mesh geometry on codend size selection. This is the first time that the theoretical link between variation in mesh geometry and size selection is addressed experimentally.

Taking the SR value estimated by the fixed-mesh codend as reference, the preliminary results presented in this report reveal that the variability in mesh geometry contributes to a significant increase in SR of about 45% for cod, while the differences in SR are not significant for flatfish species. Such results are supported by theoretical predictions based on the theoretical FISHSELECT framework (Herrmann *et al.*, 2009). Considering for example an increase in OA from 20° to 60°, the FISHSELECT framework predicts an increase of L50 of ~ 20 cm for cod (Herrmann *et al.*, 2009), while the predicted increase in flounder L50 is only of ~ 4 cm (Luschtinetz, 2012). Therefore, the lack of significance in SR values for flatfish species could be associated to a low variation in selectivity within a wide range of working OA that could be taking place during the haul.

The experiment conducted was largely conditioned by the limited number of cod catches occurred during the cruise. The significant signal detected for the SR of cod (Figure 13) was only possible due to an *ad-hoc* simplification to the original experimental plan, focusing the available sampling effort to a single pairwise codend comparison (D1 vs D2). To fully understand how the variation in mesh geometry influence size selection of trawl codends, it is essential to conduct further selectivity sea trials to conclude the experimental plan initiated, preferably fishing on the same fish populations exploited during the current 797. Solea cruise.

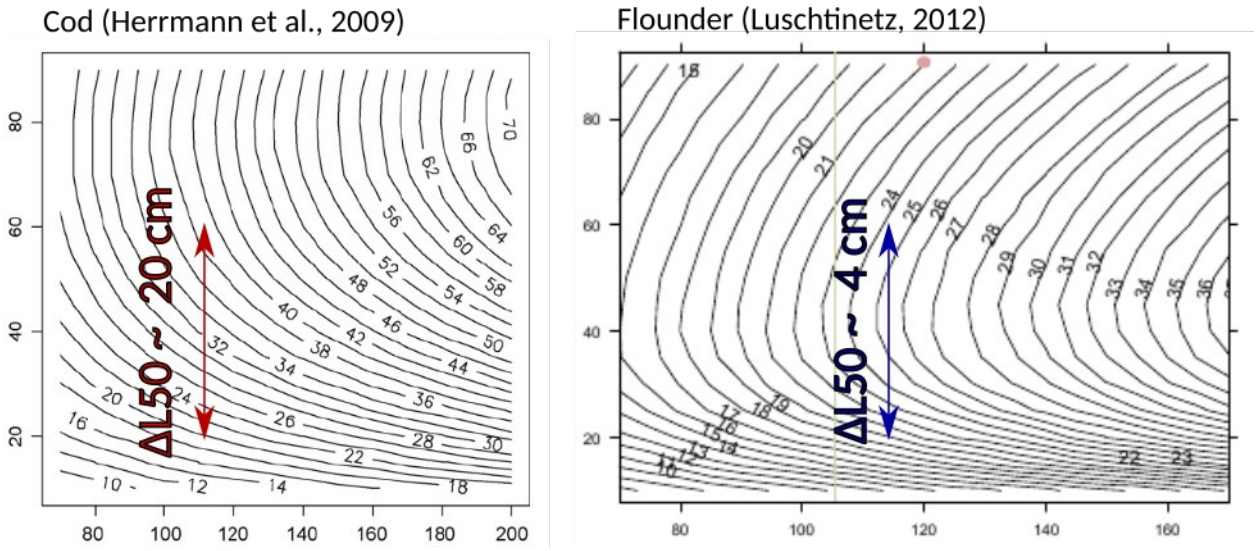

Figure 14: Isolines showing the variation of L50 (cm) for cod (left) and flounder (right) with varying mesh size (x axis) and OA (y axis). Figures extracted respectively from Herrmann et al. (2009) and Luschtinetz (2012).

5 Cruise participants

Table 3

Name	Function	Institute
Juan Santos	Cruise Leader	Thünen Inst. Baltic Sea Fisheries
Bent Herrmann	Guest researcher	DTU-Aqua (DK) / UiT (NOR)
Zita Bak-Jensen	Guest researcher	DTU-Aqua (DK)
Nadine Jacques	Guest researcher	UiT (NOR)
Beate Büttner	Technician	Thünen Inst. Baltic Sea Fisheries
Kerstin Schöps	Technician	Thünen Inst. Baltic Sea Fisheries

6 Bibliography

Akaike, H. 1974. A new look at the statistical model identification. IEEE Transactions on Automatic Control, 19: 716–723.

Fonteyne, R., Buglioni, G., Leonori, I., and O'Neill, F. G. 2007. Review of mesh measurement methodologies. Fisheries Research, 85: 279–284.

Herrmann, B. 2005. Effect of catch size and shape on the selectivity of diamond mesh cod-ends: I. Model development. Fisheries Research, 71: 1–13. Elsevier.

Herrmann, B., Frandsen, R. P., Holst, R., and O'Neill, F. G. 2007. Simulation-based investigation of the paired-gear method in cod-end selectivity studies. Fisheries Research, 83: 175–184.

Herrmann, B., Krag, L. A., Frandsen, R. P., Madsen, N., Lundgren, B., and St, K.-J. 2009. Prediction of selectivity from morphological conditions: Methodology and a case study on cod (Gadus morhua). Fisheries Research: 13.

Luschtinetz, U. 2012. Size selection of European flounder (Platichthys flesus) in the demersal Baltic cod trawl fishery – Theoretical investigations which improve multispecies selection. University of Hamburg. 86 pp.

Madsen, N. 2007. Selectivity of fishing gears used in the Baltic Sea cod fishery. Reviews in Fish Biology and Fisheries, 17: 517–544.

Millar, R. B. 1993. Incorporation of between-haul variation using bootstrapping and nonparametric estimation of selection curves. Fisheries Bulletin, 91: 564–572.

Millar, R. B., and Fryer, R. J. 1999. Estimating the size-selection curves of towed gears, traps, nets and hooks. Reviews in Fish Biology and Fisheries, 9: 89–116.

Pichot, G., Germain, G., and Priour, D. 2009. On the experimental study of the flow around a fishing net. European Journal of Mechanics - B/Fluids, 28: 103–116.

Pope, J., Akyüz, E., Hamley, J., and Margetts, A. 1975. Selectivity of fishing gear. Food and Agriculture Org.

Sistiaga, M., Herrmann, B., Grimaldo, E., and Larsen, R. 2010. Assessment of dual selection in grid based selectivity systems. Fisheries Research, 105: 187–199. Elsevier.

Wienbeck, H., Herrmann, B., Moderhak, W., and Stepputtis, D. 2011. Effect of netting direction and number of meshes around on size selection in the codend for Baltic cod (Gadus morhua). Fisheries Research, 109: 80–88.

Wienbeck, H., Herrmann, B., Feekings, J. P., Stepputtis, D., and Moderhak, W. 2014. A comparative analysis of legislated and modified Baltic Sea trawl codends for simultaneously improving

the size selection of cod (Gadus morhua) and plaice (Pleuronectes platessa). Fisheries Research, 150: 28–37.

Wileman, D. A., Ferro, R. S. T., Fonteyne, R., and Millar, R. B. 1996. Manual of methods of measuring the selectivity of towed fishing gears. ICES Cooperative Research Report N° 213. International Council for the Exploration of the Sea (ICES).

Table 4: Summary of hauls conducted in the first part of the cruise. Catch weight (kg) by species or group of species combining test and cover included (PLE=plaice, FLE = Flounder, WIT=Withing, OTHERS= other fish species, MIX = invertebrates and algae combined).

Date	haul	Valid	Design	Lat	Lon	Course	Depth	Speed	Duration	COD	WIT	DAB	PLE	FLE	OTHERS	MIX
2021/09/16 06:36:49	1	Y	OA40	54°12.2	11°59.0	264	15	4	15	0	0	8.83	4.95	1.14	0	2.52
2021/09/16 08:01:57	2	Y	OA40	54°12.0	11°59.8	266	15	3	25	0.02	0	103.34	50.29	8.62	0.78	4.57
2021/09/16 10:27:03	3	Y	OA40	54°12.2	11°49.0	281	20	4	20	0	0	5.64	0.85	0.37	0.04	7.3
2021/09/16 13:45:47	4	Y	OA40	54°11.7	11°55.6	54	17	4	20	0	0	19.53	11.53	5.84	0.15	2.93
2021/09/17 05:37:12	5	Y	OA40	54°36.3	13°43.1	152	26	5	20	0.47	0.02	0.61	4.33	28.29	3.1	16.88
2021/09/17 06:57:28	6	Y	OA40	54°40.5	13°47.1	32	32	4	20	1.33	0.1	0.43	40.55	120.86	6.4	0.27
2021/09/17 10:08:28	7	Y	OA40	54°50.0	13°47.6	306	44	4	15	0.38	0	0.99	20.97	37.04	5.61	0.34
2021/09/17 12:42:08	8	Y	OA40	54°58.7	13°54.1	270	46	4	15	2.01	0.89	0	15.37	8.61	4.35	0.88
2021/09/17 13:57:50	9	Y	OA40	54°59.6	13°41.9	279	46	4	30	0.36	0	0.61	68.15	49.75	7.44	2.85
2021/09/18 05:36:35	10	Y	OA40	54°25.2	12°19.4	37	19	4	15	0.14	0	5.58	5.08	1.98	0.94	8.85
2021/09/18 06:37:40	11	Y	OA40	54°24.4	12°13.3	213	17	4	15	0.47	0	71.42	101.76	2.52	4.77	3.33
2021/09/18 08:39:36	12	Y	OA40	54°11.8	11°55.8	238	17	4	15	0	0	6.13	4.79	0.18	0	7.52
2021/09/18 10:11:57	13	Y	OA40	54°12.2	11°48.7	293	21	5	20	0	0	1.54	0.33	0.24	0	4.88
2021/09/18 11:37:07	14	Y	OA40	54°17.2	11°55.0	25	19	4	20	0	0	4.86	0.2	0.39	0.04	4.16
2021/09/18 14:41:06	15	Y	OA40	54°34.1	12°24.5	50	18	4	15	0.18	0.01	22.54	13.06	2.66	0.21	39.02
2021/09/19 05:34:22	16	Y	OA40	54°32.1	13°48.0	7	20	5	20	2.32	0	0.71	3.04	29.36	1.49	27.93
2021/09/19 06:43:16	17	Y	OA40	54°29.9	13°44.8	90	18	4	20	4.02	0.27	0	3.02	14.94	3.55	15.97
2021/09/19 08:07:49	18	Y	OA40	54°30.7	13°57.5	127	17	4	20	0.16	0	0	1.05	14.34	4.51	0.63
2021/09/19 10:12:51	19	Y	OA40	54°21.0	14°00.7	75	14	4	20	0	0	0	1.1	20.77	1.62	1.18
2021/09/19 12:08:55	20	Y	OA40	54°29.7	13°47.4	280	18	4	35	5.14	0	0	2.99	24.71	4.4	20.78
2021/09/20 05:35:10	21	Y	OA40	54°29.8	13°44.3	93	18	4	35	3.76	0	0	3.82	19.99	6.77	20.72
2021/09/20 07:04:39	22	Y	OA40	54°32.4	13°48.0	6	21	3	60	2.11	0.05	0	55.73	61.88	6.08	61.68
2021/09/20 10:09:37	23	Y	OA40	54°29.8	13°44.4	93	18	4	45	2.27	0	0	7.41	36.58	4.48	22.38
2021/09/20 11:21:25	24	Y	OA40	54°29.8	13°48.4	275	18	4	50	3.15	0	0	6.49	51.73	4.25	40.2
2021/09/20 12:36:23	25	Y	OA40	54°29.8	13°44.0	98	19	4	50	29.34	0	0	2.7	62.6	4.53	46.5
2021/09/21 05:35:19	26	Y	T0	54°29.8	13°43.9	93	20	4	50	2.78	0	0.02	9.48	121.16	12.73	63.88
2021/09/21 07:08:54	27	Y	T0	54°33.5	13°48.1	329	22	4	30	2	0.42	0.06	8.79	92.23	8.53	58.84
2021/09/21 10:10:49	28	Y	T0	54°29.7	13°44.0	87	19	4	50	2.01	0.09	0	5.28	68.54	7.88	34
2021/09/21 11:36:31	29	Y	T0	54°29.8	13°48.3	267	18	4	50	5.12	0	0	4.62	47.42	5.18	36.62
2021/09/21 13:37:07	30	Y	T0	54°29.9	13°44.0	93	19	4	50	1.69	0	0	5.15	70.84	10.44	20.54
2021/09/22 05:37:59	31	Y	T0	54°52.6	13°19.3	272	44	4	30	0.15	0.21	13.64	67.41	56.9	10.41	6.27
2021/09/22 06:59:36	32	Y	T0	54°48.3	13°15.0	264	43	4	30	0.2	0.34	18.01	96.91	103.82	7.47	2.21
2021/09/22 10:09:06	33	Y	T0	54°40.2	13°05.0	294	19	4	15	0.26	0	3.56	11.8	7.56	1.74	15.74
2021/09/22 12:02:04	34	Y	T0	54°38.7	12°41.9	233	19	4	30	0.33	0.08	24.27	76.25	3.41	2.07	1.82
2021/09/22 14:11:32	35	Y	T0	54°26.4	12°20.7	213	19	4	20	0.02	0	22.17	15.86	2.37	0.03	10.31

Table 4: Summary of hauls conducted in the first part of the cruise. Catch weight (kg) by species or group of species combining test and cover included (PLE=plaice, FLE = Flounder, WIT=Withing, OTHERS= other fish species, MIX = invertebrates and algae combined).

Date	haul	Valid	Design	Lat	Lon	Course	Depth	Speed	Duration	COD	WIT	DAB	PLE	FLE	OTHERS	MIX
2021/09/25 06:04:18	36	Y	T0	54°12.2	11°59.9	273	15	4	20	0.04	0.02	6.83	71.4	2.34	7.42	1.65
2021/09/25 07:19:00	37	Y	T0	54°14.6	11°47.7	271	24	4	20	0.02	0	0.54	4.15	1.5	1.34	4.93
2021/09/25 13:16:50	38	Y	T0	54°54.3	12°55.3	73	33	4	20	0.75	0.09	12.55	74.05	17.05	2.53	1.11
2021/09/25 14:11:57	39	Y	T0	54°54.2	12°59.5	44	40	4	20	5.49	0.17	18.24	162.15	62.63	4.51	0.99
2021/09/26 05:33:17	40	Y	T0	54°29.8	13°44.4	89	18	4	20	1.95	0.1	0.72	8.31	23.02	2.23	33.28
2021/09/26 06:23:21	41	Y	T0	54°29.9	13°43.9	93	20	5	40	6.15	0.05	0.03	6.89	59.99	12.61	37.54
2021/09/26 07:56:14	42	Y	T0	54°29.8	13°48.2	267	18	4	50	0.93	0	0.51	5.99	67.36	6.14	67.13
2021/09/26 10:10:11	43	Y	T0	54°35.7	13°48.1	177	22	4	50	4.85	0.02	0.48	84.47	62.16	5.53	161.42
2021/09/26 12:06:40	44	Y	T0	54°29.9	13°43.9	95	20	4	50	1.95	0.02	0	13.42	69.57	5.86	99.22
2021/09/27 05:34:08	45	Y	T0	54°36.3	13°44.9	135	26	4	50	5.52	3.78	0.15	51.51	103.97	8.23	26.49
2021/09/27 07:19:37	46	Y	T0	54°29.8	13°44.0	86	19	3	50	2.17	0.22	0.14	11.68	136.37	5.73	154.76
2021/09/27 10:10:16	47	Y	T0	54°29.8	13°43.7	89	23	4	50	6.61	0.17	0.39	5.79	72.71	2.92	65.22
2021/09/27 11:23:52	48	Y	T0	54°29.9	13°48.2	250	18	4	50	1.76	0	0	3.7	65.84	2.63	90.04
2021/09/28 05:35:06	49	Y	OA40	54°29.8	13°44.3	97	18	4	40	3.53	0.06	0	6.19	58.69	5.98	120.47
2021/09/28 07:14:59	50	Y	OA40	54°29.8	13°58.8	317	17	4	60	1.22	0	0	33.07	90.06	4.53	4.2
2021/09/28 10:10:02	51	Y	OA40	54°29.8	13°44.2	92	18	4	50	1.84	0	0.17	8.74	72.58	3.42	79.29
2021/09/28 11:27:01	52	Y	OA40	54°29.8	13°48.7	258	18	4	50	2.43	0	0	5.06	71.44	5.05	71.31
2021/09/28 12:42:11	53	N	OA40	54°29.7	13°44.1	84	19	4	50	3.43	0.04	0	5.13	50.47	4.16	54.68
2021/09/29 04:56:38	54	Y	OA40	54°29.9	13°44.2	101	19	4	50	4.77	0.09	0	8.64	20.52	4.76	79.12
2021/09/29 06:10:13	55	Y	OA40	54°29.8	13°48.4	264	18	4	50	3.01	0	0	0	0	0	0